26

Carbon Nanotubes in Bone Tissue Engineering

Kaveh PourAkbar Saffar[1,2] , Nima JamilPour[3] and Gholamreza Rouhi[4]
[1]*Department of Biomedical Engineering, Amirkabir University of Technology, Tehran, Iran*
[2]*Department of Mechanical and Manufacturing Engineering, University of Calgary, Calgary, Alberta, Canada*
[3]*School of Mechanical Engineering, Semnan University, Semnan, Iran*
[4]*Department of Mechanical Engineering and School of Human Kinetics, University of Ottawa, Ontario, Canada*

1. Introduction

Exceptional properties of carbon nanotubes (CNTs) such as electrical, mechanical, chemical and thermal, attract growing attention and interest among different disciplines toward their usage in modern technologies. A more recent implementation of the concept is encountered within the field of bioengineering where researchers are focusing on the bioactivity and biocompatibility of CNTs. Carbon is the main component of biomolecules, and this makes CNT to be considered as a biocompatible material. Several studies report increase in the activity of living cells adjacent to CNTs. Electrical response of CNTs to mechanical loading makes them piezoelectric biosensors. Having the highest strength known so far, CNTs are believed to be an ideal reinforcement for composites. Use of such versatile functions of carbon nanotubes, as composite matrix reinforcements, may have the potential to apply this unique nano-structured material to tissue engineering issues such as replacement, healing, and growth (Abarrategi et al., 2008). At the same time, cell adhesion, viability, and accelerated growth support the idea of using CNTs as substrates for tissue regeneration (Lobo et al., 2008). These potentials and many others point at the suitability of CNTs for bone tissue engineering applications (Usui et al., 2008). For example, CNTs can be viewed as reinforcement to orthopedic materials such as bone cement (Marrs et al., 2006; 2007). It has also the ability to act as a biosensor to report bone growth adjacent to an implant (Sirivisoot & Webster, 2008). Having a density similar to graphite and much lower than that of other metallic bone scaffold materials, CNTs have been viewed as excellent stimulant scaffolds for growth and proliferation of osteoblasts, the bone forming cells (Zanello et al., 2006). Therefore, bone regeneration on CNT reinforced scaffolds is increasingly favored. This suggests making a mechanically enhanced nano-bio-composite for applications in both curative and preventative approaches in bone tissue engineering.
In this chapter, first, a brief explanation about the bone structure as a biocomposite at different hierarchical levels and a quick review on bone mechanics and remodeling process will be provided. Next, the most important approaches to CNT applications in bone tissue engineering will be reviewed and a new area of applicable researches will be introduced.

This includes investigation on the idea of bone mineral phase formation on CNTs as a replacement for collagen fibers in the infrastructure of bone. The initial steps of such a study should include modeling and simulation of the phenomenon, since it is dealing with a living tissue and many difficulties come along with experimental studies. Therefore, modeling issues will be addressed and discussed based on the recent experimental findings on the potentials of CNT as a biocompatible reinforcement and scaffold for bone tissue growth. Some results of modeling will be presented and also some predictions of our theoretical model will be provided and discussed based on both mechanical and biological functions of bone tissue.

2. Bone Structure, Mechanics and Remodeling Process

Bone is the main constituent of the skeletal system and differs from the connective tissues in rigidity and hardness. The rigidity and hardness of bone enable the skeleton to maintain the shape of the body; to protect the vital organs; to supply the framework for the bone marrow; and also to transmit the force of muscular contraction from one part to another during movement (Cowin, 2001). It is made basically of the fibrous protein collagen, impregnated with a mineral closely resembling calcium phosphate (Currey, 2002). The mineral content of bone acts as a reservoir for ions, particularly calcium (almost 99% of the calcium of our body is stored in bone), and it also contributes to the regulation of extracellular fluid composition (Cowin, 2001). It also contains water, which is very important mechanically, some not well-understood proteins and polysaccharides, living cells and blood vessels. The organic matrix of bone consists of 90% collagen, the most abundant protein in the body, and about 10% of various noncollagenous proteins (Behari, 1991). The protein part, mainly collagen type I, forms a model for the subsequent deposition of hyroxyapatite, the mineral phase of bone which provides rigidity to the structure. From mechanical point of view, bone is a non-homogeneous and anisotropic material. Spongy and cortical bones can be considered as an orthotropic (with 9 independent material constants) and transversely isotropic materials (with 5 independent material constants), respectively. In the physiological range of loading, bone can be assumed as a linear elastic material, with negligible viscoelastic effects (Rouhi, 2006a). Bone is stronger in compression than in tension, and much greater young's moduli of elasticity than shear modulus (Bartel et al., 2006).

The term composite is usually employed for those materials in which two or more distinct phases are separated on a scale larger than the atomic, and in which their material properties such as stiffness and strength are changed compared with those of a homogeneous material. On the basis of the definition of a composite and also by considering bone structure, it is evident that bone is a composite material. Bone, as a biocomposite, shows hierarchical structures at different scales (Lakes, 1996). For example, in cortical bone, on the microstructural level, there are osteon (or havesian systems), which are large hollow fibers (200 to 250 μm outer diameter) composed of concentric lamellae and of pores. The lamellae are made up of fibers, and the fibers contain fibrils. At the nanosclae, the fibers are a composite of mineral hydroxyapatite and the protein collagen. These well organized structural features have been associated with various unique structural properties. For instance, the stiffness of bone is related to the composite structure of mineral microcrystals and collagen (mostly type I) fibers (Lakes & Saha, 1979); and the cement lines as weak interfaces convey a degree of toughness to bone (Piekarski, 1970).

Bone is produced inside the body and is usually covered with cells throughout life. Because of its nonexpendable nature, all bone resorption and formation occurs at the bone surfaces, as opposed to soft biological tissues which can have both interstitial and appositional growth. Bone is a porous structure with different values of porosity depending on its macrostructure. At the macroscopic level, there are basically two types of bone structures: cortical (compact or Haversian) and cancellous (spongy, or trabecular) bone. Cortical bone is a dense, solid mass with only microscopic channels, and with a maximal density of about 1.8 gr/cm^3. Approximately 80% of the skeletal mass in the adult human is cortical bone, which forms the outer wall of all bones and is largely responsible for the supportive and protective function of the skeleton. The main structural unit of the cortical bone is called osteon. A typical osteon is a hollow cylinder with the outer and inner diameteres of about 200 (or 250) and 50 μm, respectively. An osteon is made up of 20 to 30 concentric lamellae, and surrounding the outer border of each osteon there is a cement line, a 1-2 μm thick layer of mineralized matrix deficient in collagen fibers, which it is believed they act as crack stoppers when cracks are present. On the other hand, cancellous (spongy or trabecular) bone is a lattice of narrow rods and plates (70 to 200 μm in thickness) of calcified bone tissue called trabeculae, with an average thickness of of 100-150 μm (Van der Meulen & Prendergast, 2000). The trabeculae are surrounded by bone marrow that is vascular and provides nutrients and waste disposal for the bone cells. The symmetry of structure in cancellous bone depends upon the direction of applied loads. If the stress pattern in spongy bone is complex, then the structure of the network of trabeculae is also complex and highly asymmetric. Comparison of micrograph structures with the density maps show that low density, open cell, rod like structure develops in regions of low stress while greater density, closed cell, plate like structures occur in regions of higher density in cancellous bone (Gibson, 1985). There are no blood vessels within the trabeculae, but there are vessels immediately adjacent to the tissue. Trabecualr bone is less mineralized than cortical bone, and experimental evidence and data suggest that spongy bone is much more active in remodeling than in cortical bone (Guo & Goldstein, 1997). The major cellular elements of bone include osteoclasts (bone resorbing cells), osteoblasts (bone making cells), osteocytes (it is believed that they act as mechano-sensors), (Burger & Klein-Nulend, 1999) and bone-lining cells (inactive cells on the resting surfaces of bone). While osteoblasts and osteoclasts have opposite functions and have different developmental origins, they exhibit several parallel features, particularly with respect to their life cycles. Osteoblasts and osteoclasts are both temporary cells with relatively short life spans (Parfitt, 1995).

Skeletal development begins as mesenchymal condensations that appear early in the fetal period. These condensations ossify to form membrane bones through intramembranous ossification and cartilaginous bones through endochondral ossification. In both types of ossifications, bone formation is similar, beginning with an increase in the number of cells and fibers. The cells differentiate into osteoblasts, which lay down an unmineralized matrix, and the osteoid that mineralizes almost immediately. During growth, bone is formed in the necessary places and resorbed as needed to attain the final shape, in a process called modeling. Modeling involves resorption drifts and formation drifts that remove *or* add bone over wide regions of bone surfaces. Thus, in modeling bone resorbing and making cells act independently and at different spots. Modeling controls the growth, shape, size, strength, and anatomy of bones and joints. Collectively, modeling leads to increasing the outside cortex and marrow cavity diameters, shaping the ends of long bones. Modeling allows not only the development of normal architecture during growth, but also the modulation of this

architecture and mass when the mechanical condition changes. When bone trains exceed a modeling threshold window, the minimum effective strain, modeling in the formation mode is turned on to increase bone mass and strength, and lower its strains toward the bottom of the window. When strains remain below the modeling threshold, mechanically controlled formation drifts stay inactive. As the forces on bone increases 20 times in size between birth and maturity, modeling in the formation mode keeps making bones strong enough to keep their strains from exceeding the modeling threshold, and therefore from reaching the microdamage threshold (Jee, 2001). In the adult age, the localized and independent activities of cells in modeling, are replaced by a distributed and coordinated work of the cells, resulting in a dynamic state called remodeling process. The actual remodeling occurs in two steps: the osteoclasts attach to the bone surface, dissolve the mineral, and later the organic phase of the bone, opening a hole that is subsequently filled by a number of osteoblasts, which produce the collagen matrix and secrete a protein which stimulates the calcium phosphate deposition. This state can be shifted in favour of bone formation or resorption by mechanical stimulation, hormonal effects, nutrition, or diseases among other factors (Rouhi, 2006a). There are several reasons for the necessity of remodeling process, for examples: immature bone formed at the metaphyses is structurally inferior to mature bone; or the quality of adult bone deteriorates with time; or microcracks produced in bone by daily activity should be removed to attain a desired strength in bone; and/or ions concentration (e.g. calcium) should be adjusted to lie in an acceptable range; and, most likely, other factors that will be known in the future (Rouhi, 2006a). Assuming normal rates of adult bone remodeling, cortical bone has a mean age of 20 years and cancellous bone 1 to 4 years (Parfitt, 1983). Many diseases are related to global shift in the remodeling balance, for example: Osteoporosis, which is caused by increased osteoclast activity; Ostetrosis, which is an abnormal increase in bone density by reduced osteoclast activity, Osteopenia, which is the bone loss by decreased osteoblast activity. The treatment of these diseases is based on drugs that intend to restore the remodeling equilibrium. Most of the work on osteoporosis, probably the most important of these diseases, seems to be currently in the osteoclast inhibition side (Rodan & Martin, 2000; Teitelbaum, 2000; Rouhi et al., 2007).

An early hypothesis about the dependence of the structure and form of bones on their mechanical function was proposed by Galileo in 1638 (Ascenzi, 1993). The nature of this dependence was first described in a semi-quantitative manner by Wolff (Wolff, 1886), who stated that remodeling of bone occurs in response to physical stresses or to the lack of them - in that bone is deposited in sites subjected to stress and is resorbed from sites where there is not enough stress. Several mechanisms have been proposed to relate changes in mechanical loads to the adaptive responses in bone, including (among many others): piezoelectric and streaming potentials (Gjelsvik, 1973a,b; Pollack et al., 1984); mechanical fatigue microdamage (Frost,1960; Carter & Hayes, 1977; Carter & Cayler, 1983; 1985; Martin, 1992; 1995; Prendergast & Taylor, 1994); and extra- cellular fluid pressure gradient effects on bone cells (Cowin et al., 1991; 1995). Experimental evidence can be found in support of each of the above-mentioned mechanisms. In 1964, Frost subgrouped bone remodeling into surface and internal remodeling (Frost, 1964). Surface remodeling refers to the remodeling of bone on the external surfaces, i.e. on endosteal and periosteal surfaces. The phenomenological model for surface remodeling postulates a causal relationship between the rate of surface deposition or resorption and the strain in the surface of the bone (Cowin, 2003). On the basis of the fact that all bone resorption and formation occurs on bone free surfaces, a newly defined quantity so-called free surface density, was used instead of commonly used volume

fraction in the adaptive elasticity theory (Cowin & Hegedus, 1976) and surface remodeling equations are resulted (Rouhi et al., 2004). Interestingly, in the newly developed model of surface remodeling, one can see a strong dependency between the rate of surface bone remodeling and the geometry of bone mass distribution. It is also well accepted that bone microdamages can initiate and also accelerate bone remodeling process (Taylor et al., 2007). Introducing a microcracks factor besides bone specific surface into adaptive elasticity theory, a much more complex form of bone remodeling equation will be resulted (Rouhi et al., 2006b), in which not only the mechanical stimuli, but also their rate and history play a role in the rate of bone remodeling process.
A preliminary review on the bone structure, bone mechanics, and bone remodeling process, helps in better understanding of the bone tissue engineering problems. As the main subject of this chapter, the following section deals with most important applications of carbon nanotubes in bone tissue engineering.

3. Quick Review on CNT Applications in Bone Tissue Engineering

Polymer matrix composites have recently been the focus of attention in many researches and a considerable number of such studies are dealing with the application of biopolymers. Acrylic bone cement, namely poly methyl-methacrylate (PMMA), is an example of a common biopolymer. This is a biomaterial widely used in orthopedic surgeries as a bone filling cement, though is extremely weak in comparison with natural bone tissue regarding mechanical properties. This becomes meaningful when the stresses applied to a load-bearing bone in human daily activities are considered. Experimental and theoretical studies show that there is an increase in Young's modulus and fracture toughness of PMMA when reinforced with CNTs (Marrs et al., 2006). The resulting composite also exhibits improved fatigue and fracture resistance by bridging and arresting cracks and also absorbing energy (Marrs et al., 2007). Embedding functionalized CNTs into PMMA matrix thus improves the clinical functions of bone cement, mechanically, while chemical functional groups on CNT surface and tips can induce cross-links to the surrounding matrix material and contribute in load transfer from PMMA matrix to CNT. This leads to further enhancement of the mechanical properties of the bone cement.
Ninety-five percent of bone organic phase contains collagen (Judex et al., 1999). Collagen is a fibrous protein which exists in both soft and hard tissues, and plays a critical role in providing them with mechanical tensile strength. Although many researchers studying carbon nanotubes in collagen matrices are focusing on CNTs as scaffolds for muscle tissue engineering, the approach is most likely applicable in the area that is dealing with bone tissue. Scanning electron microscopy (SEM) observation shows physical interactions between CNT and collagen matrix, after mixing solubilized Type I collagen with the solution of carboxyl functionalized CNTs at different concentrations (MacDonald et al., 2005). Type I collagen is an interesting biomolecule that has self-assembly properties and thus may be useful in inducing assembly and alignment of CNTs. Through applying mechanical strains, the mechanism of self-assembly and alignment offers possible production of ordered and anisotropic CNT composite materials (Voge et al., 2008). This, beside proven cell viability on such a scaffold, offers utilities of the composite for various medical applications.
Bone, itself, in many studies is considered as a fiber reinforced ceramic matrix composite material for modeling purposes (Raeisi Najafi et al., 2007a,b; 2009). The complicated

structure of bone should provide high strength, for body support, and go through the remodeling process in response to applied stresses caused by everyday normal and/or strenuous physical activity. Bone should also be porous so that oxygen and other nutrients can be available for internal cells, while, at the same time, this porosity must not reduce its resistance to fracture. Bone is also a main reservoir of minerals in the body. It is a composite of minerals, organics, and water. The fundamental nano-structure of bone is mineralized collagen. Type I collagen fibril (organic phase) in bone is made up of three polypeptide chains of amino acids in a triple helix. Such a triple-helical molecule can be viewed as a fiber with 1.5 nm in diameter and 300 nm in length. This stiff protein provides tensile strength of bone and is the main component of the matrix in which the mineral phase forms. Mineral component of bone is dahllite, or carbonated apatite $(Ca_{10}(PO_4, CO_3)_6(OH)_2)$, in the form of plate-shaped crystals of 50×25 nm, and a third dimension of about 1.5 to 4 nm. Long axis of the plate is generally parallel to bone axis, maximizing its compressive strength (Weiner & Wagner, 1999; Meyers et al., 2008).

Hydroxyapatite (HAp), with a chemical formula of $(Ca_{10}(PO_4)_6(OH)_2)$ is a bioceramic material, often used for clinical bone grafting and implantation. HAp has the ability to bond chemically with living bone tissue because of its chemical, compositional, biological, and crystal structure similarities to native apatite, bone mineral phase, in the human skeleton. Furthermore, the bioactivity and biocompatibility of HAp inspire osteoblast adhesion and proliferation (Rabiei et al., 2007). However, brittle HAp is fragile in tension and offers low fracture toughness in comparison with natural bone, and thus is unsuitable for main load bearing sites. On the other hand, excellent mechanical and biological characteristics of CNTs suggest the chance of strengthening and toughening HAp, while keeping its bioactivity (White et al., 2007). Measurements on HAp-CNT composite coatings fabricated by laser surface alloying show increase in elastic modulus and hardness of HAp due to adding CNT (Chen et al., 2006). Scratching tests also indicate enhanced wear resistance and lower friction coefficient as a result of raising the amount of CNTs in the composite (Chen et al., 2007). Therefore, HAp-CNT composite is introduced as a favorable coating material for load-bearing metallic implants. Bending strength and fracture toughness of sintered HAp-CNT composite is reported to improve compared to pure HAp (Li et al., 2007). Scattered CNTs in HAp coating by plasma spraying method, result in promotion of fracture toughness and crystallinity of the composite. Higher crystallinity leads to enhanced precipitation of apatite over the CNT surface, observed by SEM. Moreover, unlimited growth of cultivated human osteoblast cells is also detected near the CNT surface (Balani et al., 2007).

CNTs, on the other hand, can be considered as the mineralization site for HAp. Carboxyl functionalized CNTs (CNT–COOH) are used to chemically synthesize HAp, as an effective template. This is due to the capability of carboxylate ions (COO^-) to absorb calcium ions (Ca^{2+}) and contribute in HAp crystallization as a result of exposure to phosphate ions (PO_4^{3-}) (Aryal et al., 2006a). The method is also examined using simulated body fluid to provide physiological conditions. These synthesized composites are found to chemically resemble natural bone. Initiation of HAp nucleation is shown (by physico-chemical characterization of the composites) to take place within carboxyl group (Aryal et al., 2006b).

Other chemically functionalized CNTs are shown to be capable of conducting the scaffold role for artificial bone material growth, as well. Nucleation and crystallization of HAp is observed on functionalized CNTs with phosphonates and poly amino-benzene sulfonic acid

in the solution phase. Mineral ions attracted to these functional groups on CNTs can lead to enhanced HAp self-assembly compared to carboxylated CNTs (Zhao et al., 2005).
CNTs are close in size to the triple helical collagen fibrils which can act as templates for nano-sized HAp crystallization when functionalized and are also capable of providing structural tensile strength to the HAp-matrix composite material. However, due to the differences in mechanical behavior of CNTs and collagen fibers under loading, there is a serious necessity to look into the mechanical response of such an artificial bone nano-composite to physiological loading for possible future applications. It is consequently essential to prepare a mechanical model of CNT reinforced HAp. The model can be utilized to obtain a preliminary evaluation of the suitability of such an artificial bone tissue under physiological loading conditions.
In the following section, therefore, a model for the HAp-CNT composite is provided by incorporating cross-links which represent the bonds between CNT (reinforcement) and HAp (matrix) through functionalized sites. The cross-links are taken to be responsible for load transfer between the two phases of the composite. This model is to provide preliminary predictions for effective Young's modulus of HAp-CNT composite. The model can also be developed to predict tensile axial strength and consequently the energy absorbed prior to fracture (fracture toughness) of the CNT reinforced bone tissue.

4. Establishment of the Model

In the presented model, carboxylated CNT is considered as the substratum on which the bone mineral phase, i.e. HAp, forms. To explore the model, first, a brief description of the mechanism of HAp formation on this scaffold is required. The carbon atom of the carboxyl group (–COOH) is attached to a carbon atom on the CNT which already has three sp^2 covalent bonds with three adjacent carbon atoms on the CNT surface. This happens while the hybridization of the carbon atom on the CNT bonded to the carbon atom on functional group changes to sp^3 (Odegard et al., 2005). Therefore, carboxyl group attaches to the CNT through a sp^3 carbon-carbon (C-C) bond (see Fig. 1).

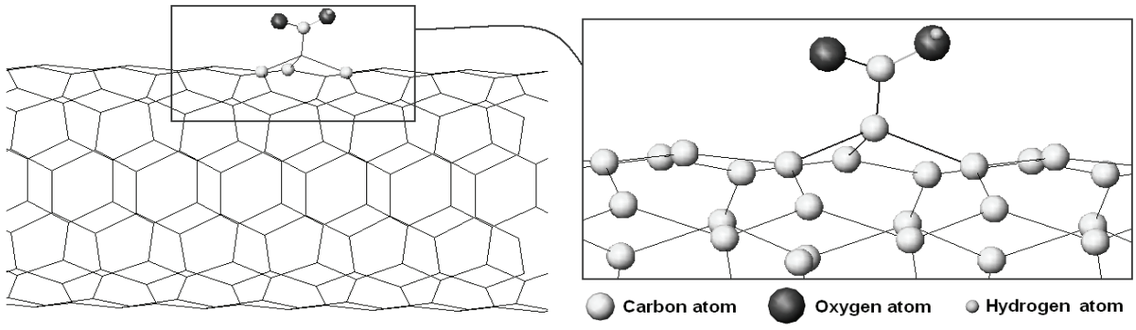

Fig. 1. Illustration of a –COOH functional group on CNT surface (PourAkbar Saffar et al., 2009a)

Carboxyl group loses hydrogen and obtains a negative electrical charge. The negative charge is evenly distributed on the two remaining oxygen atoms, causing an unstable configuration. This negative charge is tending to attract positively charged calcium ions. After that, by exposing this unstable assemblage to phosphate and hydroxide ions, it is anticipated to form a similar type of calcium phosphate to what is called HAp on the CNT

surface through the carboxyl functionalized site. This mechanism is believed to be responsible for the initiation of HAp precipitation on CNT surface (Aryal et al., 2006a,b). The calcium phosphate–like material induces ionic interaction with –COO's head due to oppositely charged ions at the contact sites. Further supply of mineral ions can lead to growth of the HAp in different directions. Other probable functional sites on the CNT may also contribute simultaneously in local HAp deposition on the CNT and this, in turn, will result in the formation of a homogeneous and continuous mineral material surrounding the CNT (see Fig. 2).

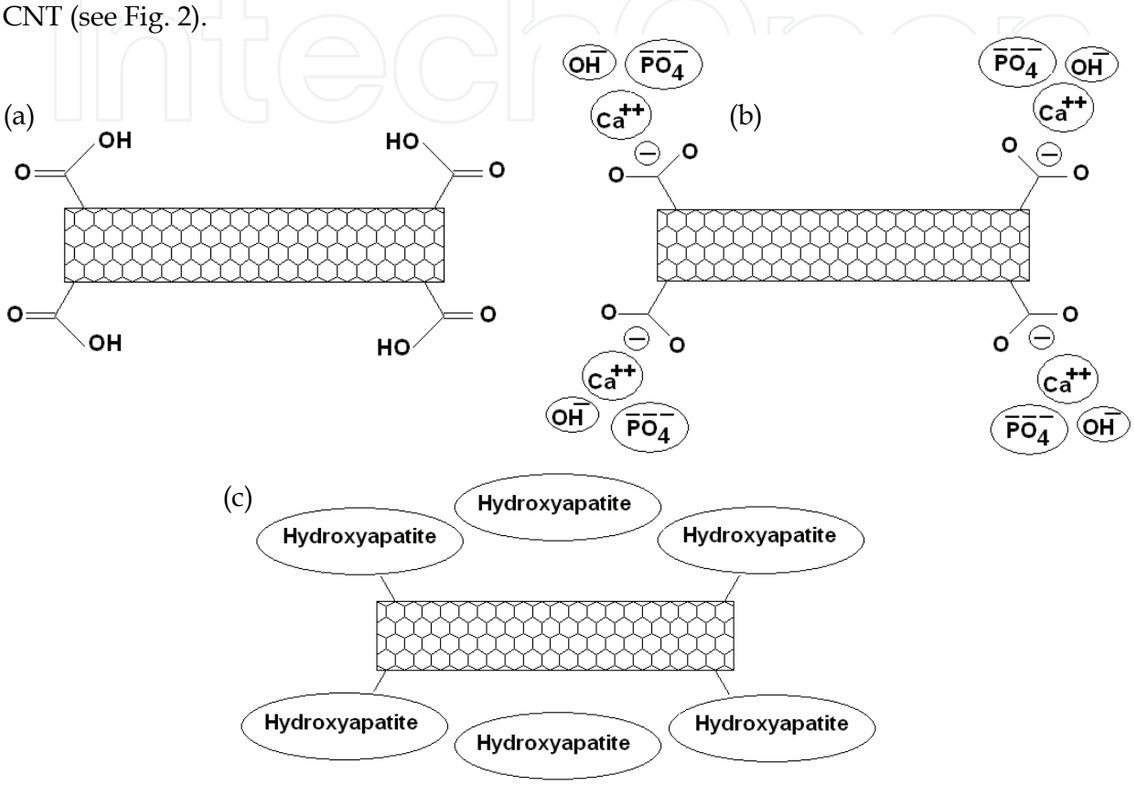

Fig. 2. (a) –COOH functionalized CNT; (b) Attraction of calcium, phosphate, and hydroxide ions; and (c) HAp formation around CNT (PourAkbar Saffar et al., 2009a)

To derive the model, a representative volume element (RVE) of the CNT-HAp composite is considered. For building the RVE, a tip-functionalized (carboxylated) armchair (8,8) single walled carbon nanotube (SWCNT) with a length of 2L is assumed onto which the HAp matrix is assembled. The CNT is considered as an elastic cylindrical beam element with a diameter of 1.08 nm for (8,8) SWCNT, at the center of the RVE. Two C–C covalent bonds are assumed at the two tips of the RVE, inducing bonding between CNT and HAp matrix. They are presented as elastic beam elements, referred to as cross-links, using a structural mechanics approach introduced by (Li & Chou, 2003). Each cross-link has total strain energy equal to the C–C bonding energy in sp^3 hybridization. Since electrostatic interactions within an ionic solid are strong enough, the ionic bonding area between carboxylate ion and HAp phase is taken as a continuous region in the model. HAp matrix in the RVE is, thus, assumed as a homogeneous, continuous hollow cylindrical beam element, and concentric with the CNT. The C–C bond length is taken to be 0.1522 nm (Cornell et al., 1995) (Fig. 2).

Outer diameter of this element is determined according to the CNT volume fraction in the RVE.

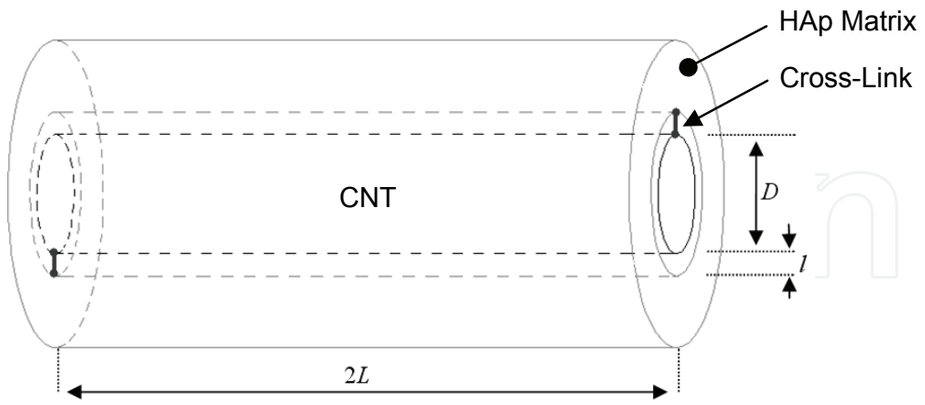

Fig. 3. RVE of HAp formed on tip-functionalized CNT

The cross-link is responsible for stress transfer from HAp matrix to the CNT, and thus, takes part in the reinforcing mechanism in the composite when subjected to an axial load. Elastic constants for CNT and HAp are indicated in Table 1.

	Young's Modulus (GPa)	Poisson's Ratio
SWCNT	1010	0.28
HAp Matrix	130	0.3

Table 1. Elastic constants of SWCNT and HAp matrix

For evaluating the characteristics of cross-link beam element, a connection between molecular and structural continuum mechanics is used. The method has been previously applied for simulating SWCNTs as space-frame structural elements, where covalent bonds are treated as beam elements. In this approach, the total atomic bonding energy in the C-C covalent bond is set equal to total strain energy of a uniform beam with length l and circular cross-sectional area A (Tserpes & Papanikos, 2005). If relatively negligible electrostatic forces and non-bonding interactions are discarded, the total bonding energy can be expressed as:

$$U_{total} = \sum U_r + \sum U_\theta + \sum U_\tau \tag{1}$$

U_r, U_θ, and U_τ are the energies due to stretch, bending, and sum of dihedral angle and out-of-plane torsion interactions, respectively. If the bond stretching increment, the bond angle variation, and the angle variation of bond twisting are represented by Δr, $\Delta\theta$, and $\Delta\phi$, respectively, then each energy can be expressed as:

$$U_r = \frac{1}{2}k_r(\Delta r)^2, \qquad U_\theta = \frac{1}{2}k_\theta(\Delta\theta)^2, \qquad U_\tau = \frac{1}{2}k_\tau(\Delta\phi)^2 \tag{2}$$

where in molecular mechanics, k_r, k_θ, and k_τ represent the resistance force constants for the bond stretching, bending, and torsion, respectively. So, direct relationships between molecular and structural mechanics parameters can be determined as:

$$\frac{EA}{l} = k_r, \qquad \frac{EI}{l} = k_\theta, \qquad \frac{GJ}{l} = k_\tau \tag{3}$$

Here, E and G are the Young's modulus and shear modulus of elasticity for the beam element. Cross-sectional area, moment of inertia, and polar moment of inertia, for a cylindrical beam with a diameter of d can be obtained as $A=\pi d^2/4$, $I=\pi d^4/64$, and $J=\pi d^4/32$, respectively. The values of molecular mechanics parameters for a C–C covalent bond in sp^3 hybridization are found to be $k_r = 4.39\times10^{-7}$ N/nm, $k_\theta = 8.76\times10^{-10}$ N.nm/rad^2, and $k_\tau = 2.78\times10^{-10}$ N.nm/rad^2 (Cornell et al., 1995; Jorgensen & Severance, 1990). Therefore, the values for d, E, and G are obtained as 0.179 nm, 2.67 TPa, and 0.42 TPa, respectively.

Once the RVE model is built as a combination of elastic elements in series and parallel orders, the problem can be tackled for axial loading condition to determine the mechanical response of the RVE in the form of elastic deformation (PourAkbar Saffar et al., 2008). This, thus, can give the effective axial Young's modulus of the RVE. Uniform axial loading causes deformation in the RVE elements. Clearly, larger deformation occurs in the element representing HAp due to its lower Young's modulus in comparison with the CNT, although this deformation is significantly smaller than non-reinforced HAp under similar loading condition. The difference in HAp and CNT deformation causes stretching in the cross-link. Therefore, cross-link participates in the reinforcing mechanism by transferring stresses from the HAp matrix to the CNT.

A criterion can be assumed for the determination of the axial tensile strength of the RVE. In this approach, the axial tensile stress applied on the RVE cross-section leads to a combination of stresses within each element, since the linking beam element transfers stresses from the matrix to the reinforcement. The resulting stresses in either HAp matrix or the C-C bond representing element may exceed the ultimate value, i.e., defined tensile strength for that element, and cause failure. Therefore, the value of axial tensile stress which causes failure in either HAp or C-C bond can be calculated as the tensile strength of the RVE (PourAkbar Saffar et al. 2009b). Here, failure of the RVE is supposed to occur without any non-linear deformations.

The effective Young's modulus defines the slope of the stress-strain curve, when neglecting the non-linear response of the chemical bonding and assuming overall linear elastic behavior for the RVE. On the other hand, the same assumption leads to the determination of the fracture strain at the point in which fracture strength is known. As a result, the area under the stress-strain curve, up to the fracture point, can be obtained as fracture toughness. This is a critical parameter which describes the energy dissipated prior to fracture.

5. Modeling Results

The head cross-linked model illustrated in Fig. 3 predicts different values of the RVE effective axial Young's modulus for various CNT volume fractions and RVE lengths (CNT aspect ratio = 2L/D). Fig. 4 illustrates plots of the Young's modulus versus CNT volume fraction for different RVE lengths. Results of current model, as seen in Fig. 4, can be compared to that of classical micromechanics models for composite materials. For the sake of comparison, Rule-of-Mixtures predictions (Voigt, 1889; Reuss, 1929), Hashin-Shtrikman upper and lower bounds (Hashin & Shtrikman, 1961a,b; 1962a,b; 1963), and Mori-Tanaka model results (Mori & Tanaka, 1973) for the composite consisting of CNT and HAp are also provided in Fig. 4.

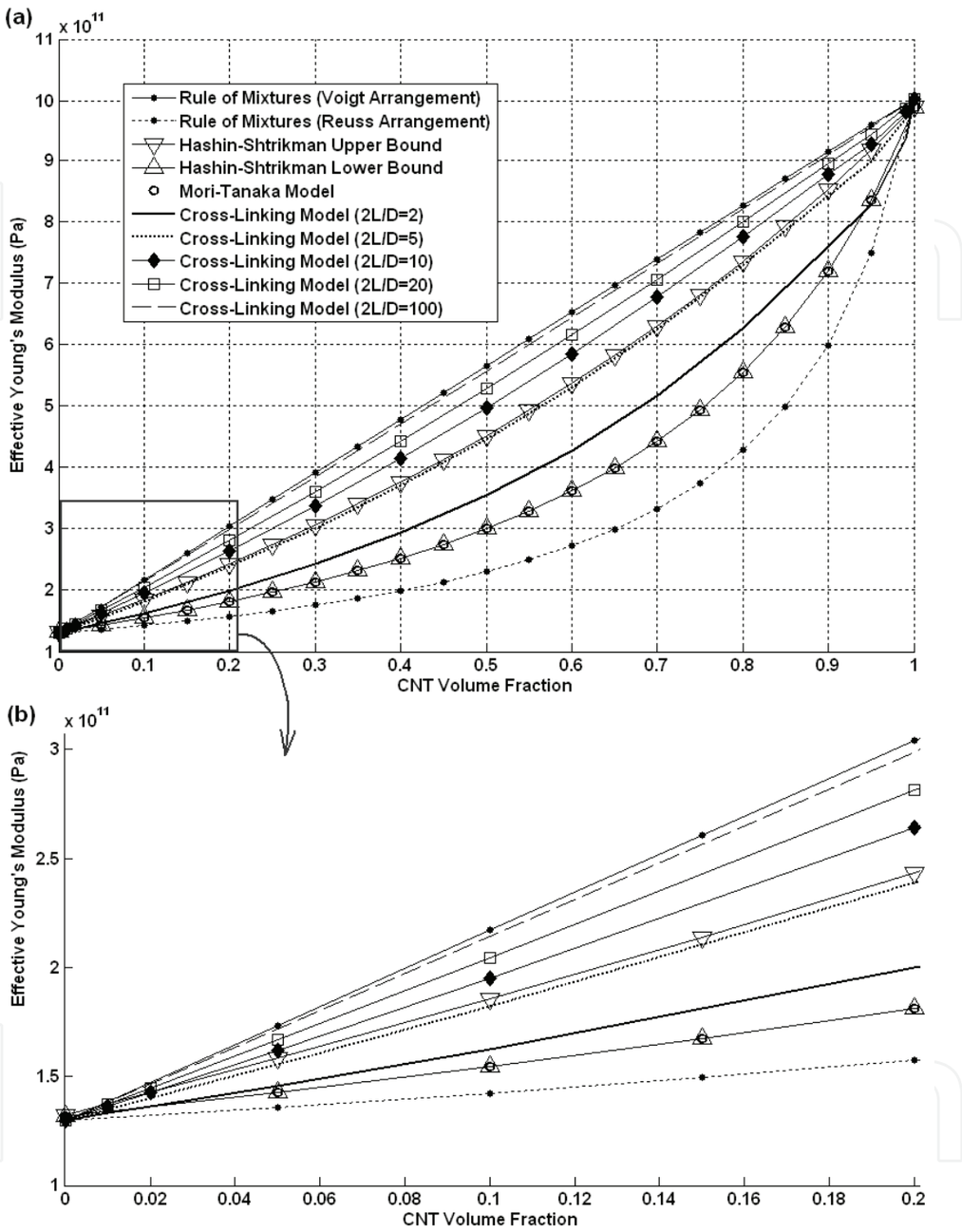

Fig. 4. RVE effective axial Young's modulus predicted by some classical models and the cross-linking model with respect to CNT volume fraction

Although primary configuration presumes head cross-linked RVEs, in an alternative configuration, this can be in the shape of additional C-C bonds with the matrix on the CNT surface, since functionalization is practically feasible on both CNT heads and sidewalls. A simple case is considered here for a RVE of a length of 10 nm, with 4 equidistance cross-links evenly distributed throughout the length. Results of the simulation for this case and

also Rule-of-Mixtures (Voigt) results for different values of CNT volume fraction (from 1 to 10%) are illustrated in Fig. 5.

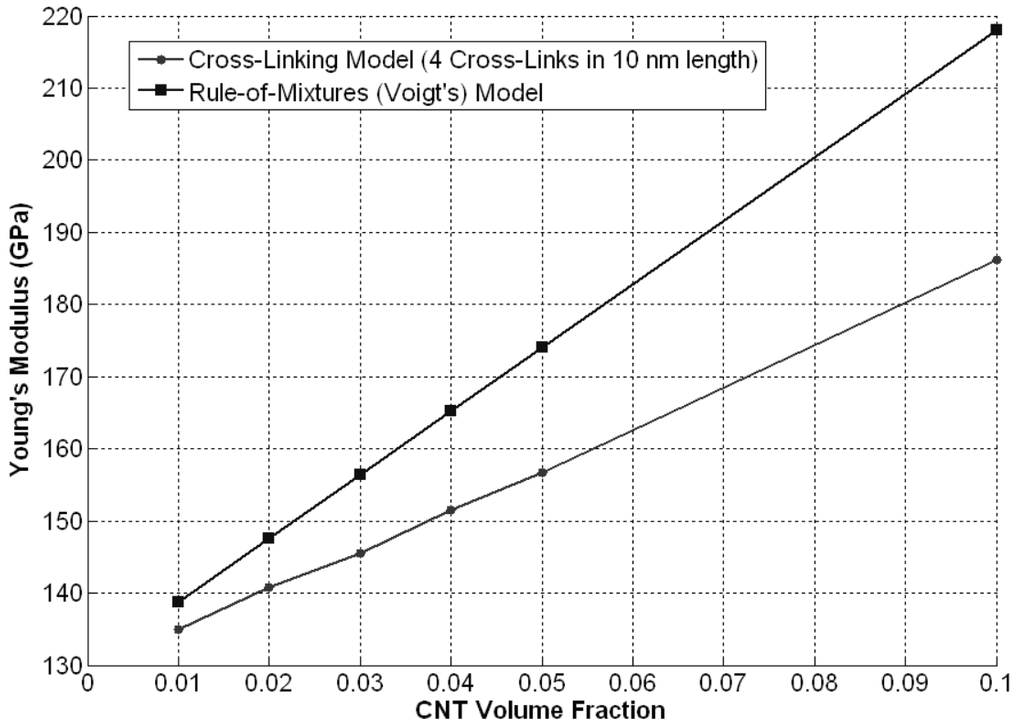

Fig. 5. Young's modulus versus CNT volume fraction predicted by Rule-of-Mixtures and the current model having 4 equidistance cross-links in 10 nm RVE length

Fig. 6 illustrates the case that cross-links are distributed in the RVE length holding equal distances of 4 nm from each other. This means that each 4 nm increase in the RVE length adds a cross-link to the RVE. This configuration is regarded for a CNT volume fraction of 10%.

Fig. 7 presents Young's moduli for two types of RVEs. The first is associated with RVEs of different length, each having only two end cross-links. The second is for the RVEs of similar lengths, having one cross-link per each 4 nm of their length. CNT volume fraction is 10% for both.

The predicted tensile strength of the RVE is shown in Fig. 8 for different CNT aspect ratios versus CNT volume fraction. This figure indicates that reinforcing mechanism acts more effectively to increase the tensile strength, when there is an increase in CNT volume fraction and/or aspect ratio.

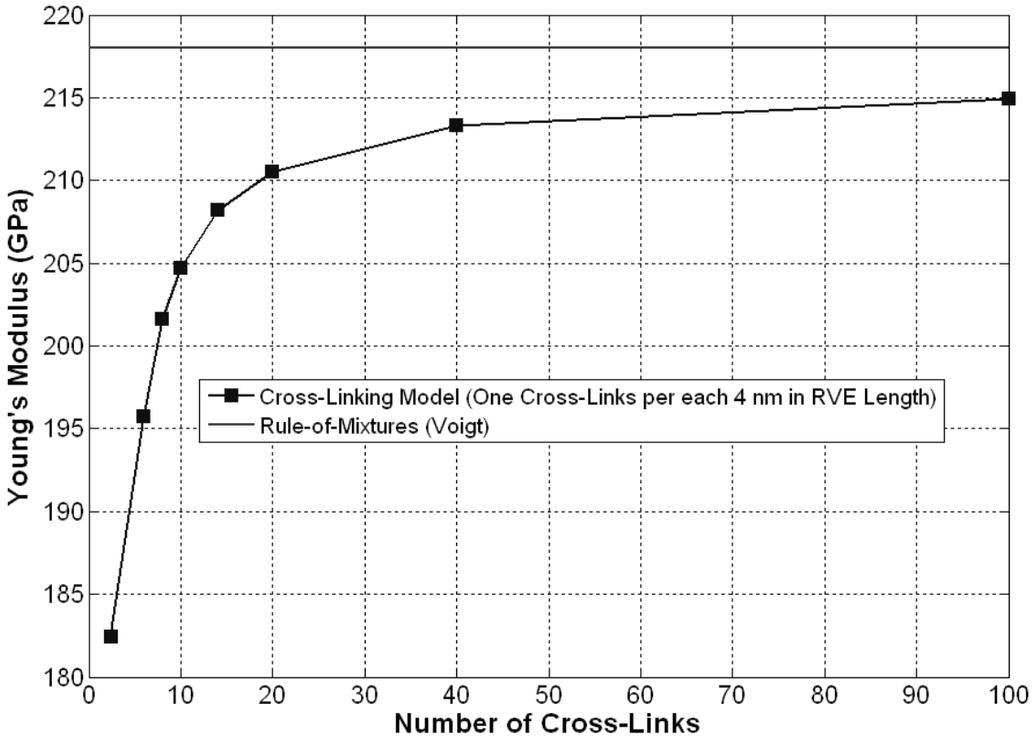

Fig. 6. Young's modulus versus number of evenly distributed cross-links in different RVE lengths (CNT volume fraction=10%)

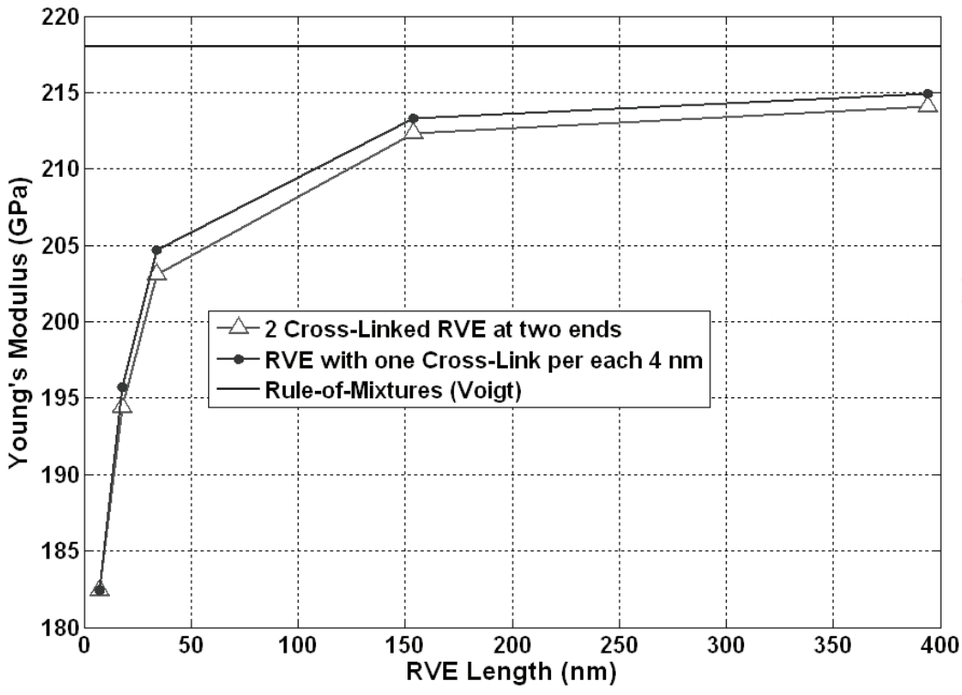

Fig. 7. Young's modulus versus RVE length (CNT volume fraction=%10)

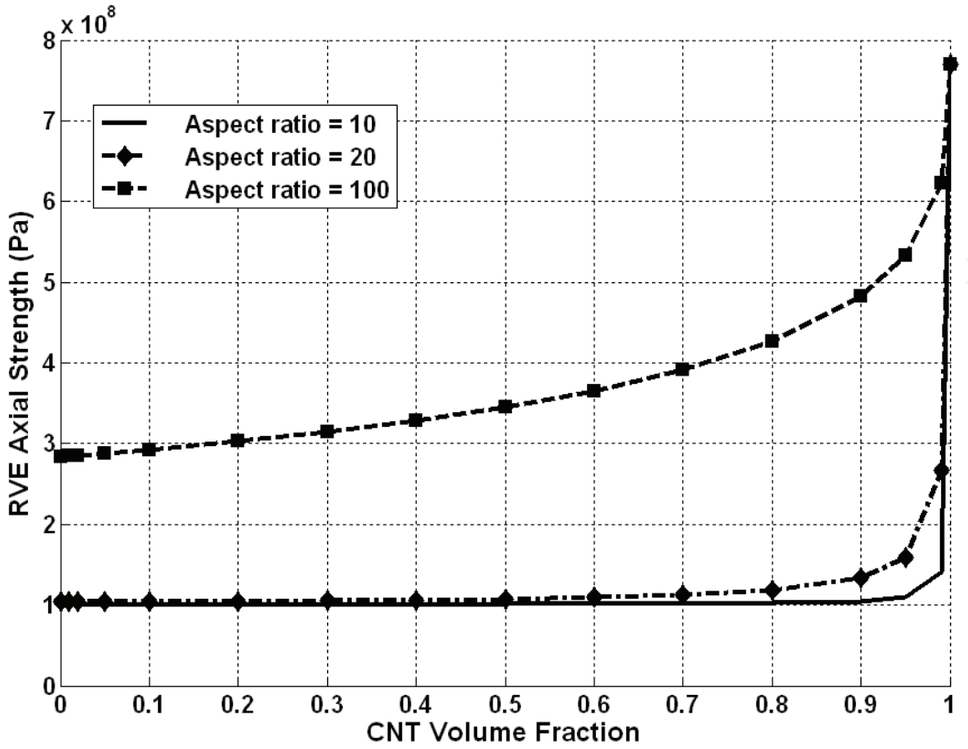

Fig. 8. Axial tensile strength versus CNT volume fraction

6. Discussions on the Model Predictions

Ordinary outputs of developed models for predicting mechanical properties of fiber-reinforced composites include consideration of microstructural Young's, shear, and/or bulk moduli with respect to volume fraction of reinforcement phase. Rule-of-Mixtures gives two general cases of isostrain and isostress arrangements of material constituents proposed by (Voigt, 1889) and (Reuss, 1929), respectively. Voigt suggests the upper limit of a range of elastic constants, while the lower limit of this range is given by Reuss's model. Results of other classical models lie between Rule-of-Mixtures estimated limits. So-called Hashin-Shtrikman upper and lower bounds (Hashin & Shtrikman, 1961a,b; 1962a,b; 1963) for the composite material behavior are the most adopted bounds for the overall properties of composites. Mori and Tanaka proposed their well-known method (Mori & Tanaka, 1973), matching Hashin-Shtrikman's lower bound for the composite behavior in certain conditions. The key point in different approaches is the pre-assumed interaction between composite phases. Voigt's model, assuming perfect bonding between matrix and reinforcement, considers isostrain condition in which deformations of the elements are equal at every contact point between the two phases. Perfect bonding assumption in such a situation, provides the uppermost limit of effective properties of the composite. However, the cross-linking model presented here, represents the inter-phase interaction only at cross-links sites which results in a significant deviation from Voigt's prediction. When interface contact is less perfect, as is the case for our cross-linking model compared to isostrain model, it is expected to see a weaker reinforcing mechanism and so a smaller value for the Young's modulus of the composite.

According to Fig. 4, the Young's modulus of the RVE of CNT-HAp predicted by the cross-linking model, lies under Voigt's model result and adjacent to Hashin-Shtrkman bounds. For a CNT aspect ratio of 5, with RVE at the same length as CNT, the cross-linking model adapts interestingly near the Hashin-Shtrikman's upper bound. It is apparent that by increasing aspect ratio, the results obtained by the current model approach those of Voigt. When the aspect ratio is approaching 100 or higher, this model's results match roughly the Voigt's prediction illustrated as a straight line in Fig. 4. This is in agreement with the general concept that increasing the CNT volume fraction and/or length leads to an improved reinforcement (Thostenson et al., 2005; Haque & Ramasetty, 2005).

The Young's modulus predicted by the present model, even for a very small aspect ratio, e.g. for a CNT aspect ratio of 2, lies above the Hashin-Shtrikman's lower bound which is also far above Reuss's prediction. This is caused by the cross-linking, and it is contrary to the isostress situation which is based on Reuss's assumption that both matrix and fibers carry the same amount of load. In the current model, however, the cross-link carries just part of the load which is caused by a combination of parallel and series elements. The phenomenon can be explained by considering the apparent difference between the Young's moduli of CNT and the matrix.

When increasing dilute volume fractions (see Figs. 4b and 5), model deviation from Voigt's prediction increases. This difference is directly related to the perfect bonding assumption in Voigt's model which results in overestimating the Young's modulus. In the cross-linking model, however, it is assumed that the only interaction between matrix and CNT is through cross-links, unlike the assumption made by Voigt, i.e., at every point throughout the contact surface there is a perfect bond between fibers and the matrix. Interesting to note that Young's moduli predicted by various models here, get closer for high CNT volume fractions; and approach a unique value when the volume fraction is 1. However, this is not of immediate interest, since empirical studies tend to concentrate on lower volume fractions of CNTs in such nano-composites (Thostenson et al., 2005; Haque & Ramasetty, 2005).

Voigt, Hashin-Shtrikman, and Mori-Tanaka models tend to predict similar curves for the Young's modulus versus volume fraction, independent of RVE lengths. The presented model, however, indicates that the longer the CNT, the more efficient the reinforcement becomes. In addition, longer CNTs have the potential to support a greater number of cross-links. The cross-linking model shows that an increase in the number of cross-links will increase the Young's modulus and in its limit will approach the value predicted by the Voigt formulation. If the number of cross-links distributed uniformly along the RVE goes to infinity, the interaction can be considered as perfect bonding. So, for such a critical condition, similar results are expected from both Voigt and the cross-linking models.

According to Fig. 6, the greater the number of cross-links, the stronger is the interaction between composite phases. The effect of increasing the CNT length, however, is much more apparent than the effect of increasing the number of cross-links in constant RVE length, as can be seen in Fig. 7. This could raise the issue of comparing the reinforcement efficiency of tip and side wall functionalized CNTs. The important point here is that adding more functional groups to the CNT surface alters the regular cylindrical shape of the CNT as a result of changes in hybridization of carbon atoms on its surface. Although the current model fails to describe this phenomenon, but on the basis of experimental observation and theoretical predictions, such modification can adversely affect nanotube properties due to induced structural defects (Balasubramanian & Burghard, 2005).

Results show a significant increase in both axial Young's modulus and tensile strength of the HAp when reinforced with CNT. A simple comparison leads to the understanding that fracture toughness of the synthesized HAp-CNT is several times higher than that of the natural bone which is structurally composed of HAp and collagen fibers (PourAkbar Saffar et al. 2009b) (see Fig. 9 as an example). Fracture toughness as a measure and indicator of the capacity of a material to resist failure, is an important parameter that can be used to determine to which category of materials, a material belongs. It is well known that pure HAp is a brittle material, while bone tissue behaves in a quasi-brittle manner (Raeisi Najafi et al., 2009), and this is due to the collagen inclusion as a flexible phase which can increase bone toughness. The enhanced elastic properties of CNTs in the HAp matrix, however, introduce the doubt on change of the material behavior as to ductile. Microcracking is a common toughening mechanism in bone, as a quasi-brittle material, which occurs near the main crack tip to resist the crack growth (Raeisi Najafi et al., 2007a,b; 2009). Moreover, it is well accepted that microcracks and microdamages in bone can initiate and accelerate bone remodeling process in which there will be a break for the crack propagation and can encourage making new bony material at the deteriorated sites (Rouhi et al., 2006; Vahdati & Rouhi, 2009). It seems reasonable, by considering the differences between the mechanical properties of the natural and artificial bone (HAp-CNTs), to assume that the rate of bone remodeling process will be altered, and possibly disturbed when CNTs replace the collagen fibers in natural bone tissue.

Assuming that CNT reinforcement increases bone fracture toughness, and decreases possibility of microcracks generation, another aspect of future researches should also be addressing whether the HAp-CNT composite is more suitable than collagen I–HAp from bone remodeling point of view or this can be seen as a drawback for the artificial bone.

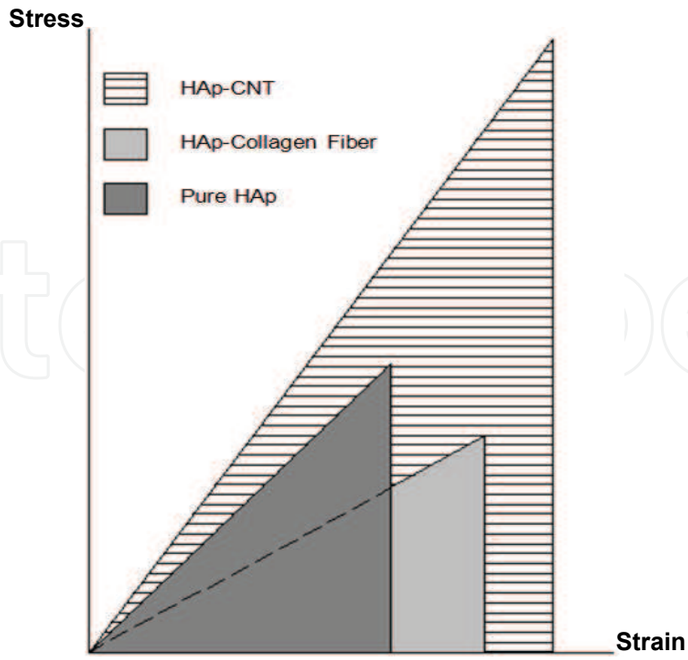

Fig. 9. Schematic stress-strain curves for HAp-CNT, HAp-collagn fiber, and pure Hap

Although promising results are shown in initial steps toward the bioapplications of CNTs as scaffolds for bone growth, more investigations need to be done to address the question of: "Is replacing collagen fibers by CNTs beneficial for bone from the bone adaptation point of view or can be seen as a disturbing factor in the remodeling process?" This study is therefore aimed at exploring the mechanical characteristics of the HAp-CNT composite in order to lay emphasize on the importance of the evaluation of the biological related effects of CNT reinforcement in such an artificial bone tissue.

7. Summary

The idea of HAp precipitation on functionalized CNTs suggests a new avenue in bone tissue engineering. For instance, implanting functionalized CNTs as solutions or substratum in the bone injury site may result in generation of the composite material. This could exemplify an appropriate application of the concept, to bone tissue therapy. A critical investigation of the applicability of CNTs as a reinforcement to a living tissue could thus find tangible potentials in preventative or post traumatic measures. This approach, however, necessitates a multidisciplinary research encompassing such subjects as Mechanical and Biomedical Engineering. The interaction between the mechanical behavior of the living tissue and the biological functions in the organism is almost totally accepted. This work is therefore aiming to evaluate such applications by exploring the mechanical properties of the HAp-CNT composite.

As the very first step in evaluating the mechanical response of the composite, a model has been presented here to obtain the effective axial Young's modulus of a RVE of HAp formed on functionalized CNT. This study predicts close behavior of the material to those suggested by classical micromechanical models. This model predicts higher Young's moduli and tensile strengths for RVEs with higher CNT contents and/or aspect ratios, as it is expected based on current knowledge of fiber composite materials. When CNT length increases, possibly, there may exist more cross-links distributed on the CNT surface in addition to those on the CNT tips, resulting in a stronger interfacial force and so bigger Young's modulus and tensile strength, as our model predicts in this study. Although initial results are promising, further careful studies are necessary to find out whether they support or cast doubt on the proposed suggestion of CNT application as bone tissue engineering scaffold.

8. Acknowledgement

Dr. A.R. Arshi from Amirkabir University of Technology, Dr. A. Raeisi Najafi from University of Illinois at Urbana-Champaign, and Dr. L. Sudak from University of Calgary are also acknowledged for collaborative supports.

9. References

Abarrategi, A.; Gutiérrez, M.C.; Moreno-Vicente, C.; Hortigüela, M.H.; Ramos, V.; López-Lacomba; J.L.; Ferrer, M.L. & del Monte, F. (2008). Multiwall carbon nanotube scaffolds for tissue engineering purposes, *Biomaterials*, Vol. 29, pp. 94-102.

Aryal, S.; Bahadur, K.C.R.; Dharmaraj, N.; Kim, K-W. & Kim, H.Y. (2006). Synthesis and characterization of hydroxyapatite using carbon nanotubes as a nano-matrix, *Scripta Materialia*, Vol. 54, pp. 131-135.

Aryal, S.; Bhattarai, S.R.; Bahadur, K.C.R; Khil, M.S.; Lee, D-R. & Kim, H.Y. (2007). Carbon nanotubes assisted biomimetic synthesis of hydroxyapatite from simulated body fluid, *Materials Science & Engineering A*, Vol. 426pp. 202-207.

Ascenzi, A. (1993). Biomechanics and Galileo Galilei, *Journal of Biomechanics*, Vol. 26, pp. 95-100.

Balani, K.; Anderson, R.; Laha, T.; Andara, M.; Tercero, J.; Crumpler, E. & Agarwal, A. (2007). Plasma-sprayed carbon nanotube reinforced hydroxyapatite coatings and their interaction with human osteoblasts in vitro, *Biomaterials*, Vol. 28, pp. 618-624.

Balasubramanian, K. & Burghard, M. (2005). Chemically functionalized carbon nanotubes. *Small*, Vol. 1, pp. 180-192.

Bartel, L.B.; Dwight T.D. & Keaveny T.M. (2006). *Orthopaedic Biomechanics Mechanics and Design in Musculoskeletal Systems*, Chap. 3, Pearson Prentice Hall.

Behari, J. (1991). Solid state bone behaviour, *Progress in Biophysics & Molecular Biology*, Vol. 56, pp. 1-41.

Burger, E.H. & Klein-Nulend, J. (1999). Mechanotransduction in bone-role of the lacuno-canalicular network, *FASEB Journal*. Vol. 13, pp. S101-S112.

Carter, D.R. & Hayes, W.C. (1977). Compact bone fatigue damage-I. Residual strength and stiffness, *Journal of Biomechanics*, Vol. 10, pp. 325-337

Carter, D.R. & Cayler, W.E. (1983). Cycle dependent and time dependent bone fracture with repeated loading, *Journal of Biomechanical Engineering*, Vol. 105, pp. 166-170.

Carter, D.R. & Cayler, W.E. (1985). A cumulative damage model for bone fracture, *Journal of Orthopedic Research,* Vol. 3, pp. 84-90.

Chen, Y.; Zhang, Y.Q.; Zhang, T.H.; Gan, C.H.; Zheng, C.Y. & Yu, G. (2006). Carbon nanotube reinforced hydroxyapatite composite coatings produced through laser surface alloying, *Carbon*, Vol. 44, pp. 37-45.

Chen, Y.; Zhang, T.H.; Gan, C.H.; & Yu, G. (2007). Wear studies of hydroxyapatite composite coating reinforced by carbon nanotubes, *Carbon*, Vol. 45, pp. 998-1004.

Cornell, W.D.; Cieplak, P.; Bayly, C.I.; Gould, I.R.; Merz, Jr. K.M.; Ferguson, D.M.; Spellmeyer, D.C.; Fox, T.; Caldwell, J.W. & Kollman, P.A. (1995). A second generation force field for the simulation of proteins, nucleic acids, and organic molecules. *Journal of American Chemical Society*, Vol. 117, pp. 5179-5197.

Cowin, S.C. & Hegedus, D.M. (1976). Bone Remodeling I: A theory of adaptive elasticity, *Journal of Elasticity*, Vol. 6, pp. 313-325.

Cowin, S.C.; Moss Salentijn, L.; & Moss, M.L. (1991). Candidates for the mechanosensory system in bone, *Journal of Biomechanical Engineering*, Vol. 113, pp. 191-197.

Cowin, S.C.; Weinbaum, S.; & Zeng, Y. (1995). A case for bone canaliculi as the anatomical site of strain generated potentials, *Journal of Biomechanics*, Vol. 28, pp. 1281-1297.

Cowin, S.C. (2001). *Bone Mechanics Handbook*, 2nd edition, CRC Press, Boca Raton, FL, USA.

Cowin, S.C. (2003). Adaptive elasticity: a review and critique of a bone tissue adaptation model, *Engineering Transactions, Polish Academy of Science*, Vol. 51 (2-3), pp. 113-193.

Currey, J.D. (2002). *Bone Structure and Mechanics*, Princeton University Press.

Frost, H.M. (1960). Presence of microscopic cracks in vivo in bone, *Bulletin of Henry Ford Hospital*, Vol. 8, pp. 25-35.

Frost, H.M. (1964). *The laws of bone Structure*; Charles C. Thomas, Springfield, IL, USA.

Gibson, L.J. (1985). The mechanical behaviour of cancellous bone, *Journal of Biomechanics*, Vol. 18, pp. 317-328.

Gjelsvik, A. (1973a). Bone remodeling and piezoelectricity-I, *Journal of Biomechanics*, Vol. 6, pp. 69-77.

Gjelsvik, A. (1943b). Bone remodeling and piezoelectricity-II. *Journal of Biomechanics*, Vol. 6, pp. 187-193.

Guo, X.E. & Goldstein, S.A. (1997). Is trabecular bone tissue different from cortical bone?, *Forma*, Vol. 12, pp. 3-4.

Haque, A. & Ramasetty, A. (2005). Theoretical study of stress transfer in carbon nanotube reinforced polymer matrix composites, *Composite Structures*, Vol. 71, pp. 68-77.

Hashin, Z. & Shtrickman, S. (1961a). Note on a variational approach to the theory of composite elastic materials, *Journal of the Franklin Institute*, Vol. 271, pp. 336-341.

Hashin, Z. & Shtrickman, S. (1961b). Note on the effective constants of composite materials, *Journal of the Franklin Institute*, Vol. 271, pp. 423-426.

Hashin, Z. & Shtrikman, S. (1962a). On some variational principles in anisotropic and nonhomogeneous elasticity, *Journal of the Mechanics & Physics of Solids*, Vol. 10, pp. 335-342.

Hashin, Z. & Shtrikman, S. (1962b). A variational approach to the theory of the elastic behavior of polycrystals, *Journal of the Mechanics & Physics of Solids*, Vol. 10, pp. 343-352.

Hashin, Z. & Shtrikman, S. (1963). A variational approach to the theory of the elastic behavior of multiphase materials, *Journal of the Mechanics & Physics of Solids*, Vol. 11, pp. 127-140.

Jee, W.S.S. (2001). Integrated bone tissue physiology: anatomy and physiology, in *Bone Mechanics Handbook* (Ed. Cowin, S.C.), Chap.1.

Jorgensen, W.L. & Severance, D.L. (1990) .Aromatic-aromatic interactions–free energy profiles for the benzene dimmer in water chloroform and liquid benzene, *Journal of American Chemical Society*, Vol. 112, pp. 4768-4774.

Judex, S.; Whiting, W. & Zernicke, R. (1999). Bone Biomechanics and Fracture, In: *Biomechanics in Ergonomics*, Kumar, S., (Ed.), Taylor & Francis, ISBN, London.

Lakes, R.S. & Saha, S. (1979). Cement line motion in bone, *Science*, Vol. 204, pp. 501-503.

Lakes, R. (1993). Materials With Structural Hierarchy, *Nature*, Vol. 361, pp. 511-515.

Li, A.; Sun, K.; Dong, W. & Zhao, D. (2007). Mechanical properties, microstructure and histocompatibility of MWCNTs/HAp biocomposites, *Materials Letters*, Vol. 61, pp. 1839-1844.

Li, C.Y. & Chou, T-W. (2005). A structural mechanics approach for the analysis of carbon nanotubes, *International Journal of Solids & Structures*, Vol. 40, pp. 2487-2499.

Lobo, A.O.; Antunes, E.F.; Machado, A.H.A; Pacheco-Soares, C.; Trava-Airoldi, V.J. & Corat, E.J. (2008). Cell viability and adhesion on as grown multi-wall carbon nanotube films, *Materials Science & Engineering C*, Vol. 28, pp. 264-269.

MacDonald, R.A.; Laurenzi, B.F.; Viswanathan, G.; Ajayan, P.M. & Stegemann, J.P. (2005). Collagen–carbon nanotube composite materials as scaffolds in tissue engineering, *Journal of Biomedical Materials Research,* Vol. 74A, pp. 489-496.

Marrs, B.; Andrews, R.; Rantell., T. & Pienkowski, D. (2006). Augmentation of acrylic bone cement with multiwall carbon nanotubes, *Journal of Biomedical Materials Research,* Vol. 77A, pp. 269-276.

Marrs, B.; Andrews, R. & Pienkowski, D. (2007). Multiwall carbon nanotubes enhance the fatigue performance of physiologically maintained methyl methacrylate–styrene copolymer, *Carbon,* Vol. 45, pp. 2098-2104.

Martin, R.B. (1992). A theory of fatigue damage accumulation and repair in cortical bone. *Journal of Orthopedic Research*, Vol. 10, pp. 818-825.

Martin, R.B. (1995). Mathematical model for repair of fatigue damage and stress fracture in osteonal bone, *Journal of Orthopedic Research*, Vol. 13, pp. 309-316.

Meyers, M.A.; Chen, P-Y.; Lin, A. & Seki, Y. (2008). Biological materials: Structure and mechanical properties, *Progress in Materials Science*, Vol. 53, pp. 1-206.

Mori, T. & Tanaka, K. (1973). Average stress in matrix and average elastic energy of materials with misfitting inclusions, *Acta Metallurgica et Materiala*, Vol. 21, pp. 571-574.

Odegard, G.M.; Frankland, S.J.V. & Gates, T.S. (2005). Effect of chemical functionalization on mechanical properties of nanotube/polymer composites, *AIAA Journal*, Vol. 43, No. 8, pp. 1828-1835.

Parfitt, A.M. (1983). The physiologic and clinical significance of bone histomorphometric data, in *Bone Histomorphometry: Techniques and Interpretation*, (Ed. Recker, R.R.), CRC Press, Boca Raton, FL, pp. 143-223.

Parfitt, A.M. (1995). Problems in the application of *in vitro* systems to the study of human bone remodeling, *Calcified Tissue International*, Vol. 56 (Suppl. 1), pp. S5-S7.

Piekarski, K.J. (1970). Fracture of bone, *Journal of Applied Physics,* Vol. 41, pp. 215-223.

Pollack, S.R.; Salzstein, R. & Pienkowski, D. (1984). The electric double layer in bone and its influence on stress-generated potentials, *Calcified Tissue International*, Vol. 36 (Suppl. 1), pp. S77-S81.

PourAkbar Saffar, K.; JamilPour, N.; Raeisi Najafi, A.; Rouhi, G.; Arshi, A.R. & Fereidoon, A. (2008). A finite element model for estimating Young's modulus of carbon nanotube reinforced composites incorporating elastic cross-links, *International Journal of Mechanical Systems Science and Engineering*, Vol. 2, No. 3, pp. 172-175.

PourAkbar Saffar, K.; Arshi, A.R.; JamilPour, N.; Raeisi Najafi, A.; Rouhi, G. & Sudak, L. (2009a). A cross-linking model for estimating Young's modulus of artificial bone tissue grown on carbon nanotube scaffold, *Journal of Biomedical Materials Research A (Submitted)*

PourAkbar Saffar, K.; JamilPour, N.; Rouhi, G.; Raeisi Najafi, A.; Arshi, A.R. & Sudak, L. (2009b). Fracture toughness of carbon nanotube reinforced artificial bone tissue, *12th International Conference on Fracture (ICF12)*, July 2009, Ottawa, Canada.

Prendergast, P.J. & Taylor, D. (1994). Prediction of bone adaptation using damage accumulation, *Journal of Biomechanics*, Vol. 27, pp. 1067-1076.

Rabiei, A.; Blalock, T.; Thomas, B.; Cuomo, J.; Yang, Y. & Ong, J. (2007). Microstructure, mechanical properties, and biological response to functionally graded HA coatings, *Materials Science & Engineering C*, Vol. 27, pp. 529–533.

Raeisi Najafi, A.; Arshi, A.R.; PourAkbar Saffar, K.; Eslami, M.R.; Fariborz, S. & Moeinzadeh, M.H. (2009). A fiber-ceramic matrix composite material model for osteonal cortical bone fracture micromechanics: Solution of arbitrary microcracks interaction, *Journal of the Mechanical Behavior of Biomedical Materials*, Vol. 2, pp. 217-223.

Raeisi Najafi, A.; Arshi, A.R.; Eslami, M.R.; Fariborz, S. & Moeinzadeh, M. (2007a). Haversian cortical bone model with many radial microcracks: An elastic analytic solution, *Medical Engineering and Physics,* Vol. 29, pp. 708-717.

Raeisi Najafi, A.; Arshi, A.R.; Eslami, M.R.; Fariborz, S. & Moeinzadeh, M.H. (2007b). Micromechanics fracture in osteonal cortical bone: A study of the interactions between microcrack propagation, microstructure and the material properties. *Journal of Biomechanics,* Vol. 40, pp. 2788-2795.

Reuss, A. (1929). Berechnung der Fliessgrenze von Mischkristallen auf Grund der Plästizitatsbedingung für Einkristalle, *Zietschrift für Angewandte Mathematik und Mechanik (Journal of Applied Mathematics and Mechanics)*, Vol. 9, pp. 49-58.

Rodan, G.A. & Martin, T.J. (2000). Therapeutic approaches to bone diseases, *Science*, Vol. 289, pp. 1508-1514.

Rouhi, G. (2006a). Theoretical aspects of bone remodeling and resorption process, *PhD Dissertation*, University of Calgary, AB, Canada.

Rouhi, G.; Firoozbakhsh, K.; Epstein, M.; Herzog, W. & Sudak, L. (2004). Free surface density instead of volume fraction in the bone remodeling equation: theoretical considerations. *Forma*, Vol. 19, Issue 3, pp. 165-182.

Rouhi, G.; Epstein, M.; Sudak, L. & Herzog, W. (2006b). Free surface density and microdamage in the bone remodeling equation: Theoretical considerations, *International Journal of Engineering Science*, Vol. 44, pp. 456-469.

Rouhi, G.; Epstein, M.; Sudak, L. & Herzog, W. (2007). Modeling bone resorption using mixture theory with chemical reactions. *Journal of Mechanics of Materials and Structures*, Vol. 2, Issue 6, pp. 1141-1156.

Sirivisoot, S. & Webster, T.J. (2008). Multiwalled carbon nanotubes enhance electrochemical properties of titanium to determine in situ bone formation, *Nanotechnology*, Vol. 19, p. 295101(12pp).

Taylor, D.; Hazenberg, J.G. & Lee, T.C. (2007). Living with cracks: Damage and repair in human bone, *Nature*, Vol. 6, pp. 263-268.

Teitelbaum, S.L. (2000). Bone resorption by osteoclasts, *Science*, Vol. 289, pp. 1504-1508.

Thostenson, E.T.; Li, C., & Chou, T-W. (2005). Nanocomposites in context, *Composites Science & Technology*, Vol. 65, pp. 491-516.

Tserpes, K.I. & Papanikos, P. (2005). Finite element modeling of single-walled carbon nanotubes, *Composites Part B*, Vol. 36, pp. 468-477.

Usui, Y.; Aoki, K.; Narita, N.; Murakami, N.; Nakamura, I.; Nakamura, K.; Ishigaki, N.; Yamazaki, H.; Horiuchi, H.; Kato, H.; Taruta, S.; Kim, Y.A.; Endo, M. & Saito, N. (2008). Carbon nanotubes with high bone-tissue compatibility and bone-formation acceleration effects, *Small*, Vol. 4, No. 2, pp. 240-246.

Vahdati, A. & Rouhi, G. (2009a). A model for mechanical adaptation of trabecular bone incorporating cellular accommodation and effects of microdamage and disuse, *Mechanics Research Communications*, Vol. 36, Issue 3, pp. 284-293.

Vahdati A.; Rouhi G.; Ghalichi, F. & Tahani, M. (2009b). Mechanically induced trabecular bone remodeling including cellular accommodation effect: A computer simulation, *Transactions of the Canadian Society for Mechanical Engineering*, Vol. 32, Issues 3-4, pp. 371-382.

Van der Meulen, M.C.H. & Prendergast, P.J. (2000). Mechanics in skeletal development, adaptation and disease, *Philosophical Transactions for the Royal Society of London A*, Vol. 358, pp. 565-578.

Voge, C.M.; Kariolis, M.; MacDonald, R.A. & Stegemann, J.P. (2008). Directional conductivity in SWNT-collagen-fibrin composite biomaterials through strain-induced matrix alignment, *Journal of Biomedical Materials Research,* Vol. 86A, pp. 269-277.

Voigt, W. (1889). Über die Beziehung zwischen den beiden Elastizitätskonstanten isotroper Körper, *Wiedmanns Annalen der Physik und Chemie*, Vol. 38, pp. 573-587.

Weiner, S. & Wagner, H.D. (1998). The material bone: structure-mechanical function relations, *Annual Reviews in Materials Science*, Vol. 28, pp. 271–298.

White, A.A.; Best, S.M. & Kinloch, I.A. (2007). Hydroxyapatite-carbon nanotube composites for biomedical applications: A review, *International Journal of Applied Ceramic Technology*, Vol. 4, pp. 1-13.

Wolff, J.L. (1886). *The law of bone remodeling*, Springer, Berlin.

Zanello, L.P; Zhao, B.; Hu, H. & Haddon, R.C. (2006). Bone cell proliferation on carbon nanotubes, *Nano Letters*, Vol. 6, pp. 562-567.

Zhao, B.; Hu, H.; Mandal, S.K. & Haddon, R.C. (2005). A bone mimic based on the self-assembly of hydroxyapatite on chemically functionalized single-walled carbon nanotubes, *Chemical Materials*, Vol. 17, No. 12, pp. 3235 -3241.

Biomedical Engineering

Edited by Carlos Alexandre Barros de Mello

ISBN 978-953-307-013-1
Hard cover, 658 pages
Publisher InTech
Published online 01, October, 2009
Published in print edition October, 2009

Biomedical Engineering can be seen as a mix of Medicine, Engineering and Science. In fact, this is a natural connection, as the most complicated engineering masterpiece is the human body. And it is exactly to help our “body machine” that Biomedical Engineering has its niche. This book brings the state-of-the-art of some of the most important current research related to Biomedical Engineering. I am very honored to be editing such a valuable book, which has contributions of a selected group of researchers describing the best of their work. Through its 36 chapters, the reader will have access to works related to ECG, image processing, sensors, artificial intelligence, and several other exciting fields.

How to reference

In order to correctly reference this scholarly work, feel free to copy and paste the following:

Kaveh PourAkbar Saffar, Nima JamilPour and Gholamreza Rouhi (2009). Carbon Nanotubes in Bone Tissue Engineering, Biomedical Engineering, Carlos Alexandre Barros de Mello (Ed.), ISBN: 978-953-307-013-1, InTech, Available from: http://www.intechopen.com/books/biomedical-engineering/carbon-nanotubes-in-bone-tissue-engineering

INTECH
open science | open minds

InTech Europe
University Campus STeP Ri
Slavka Krautzeka 83/A
51000 Rijeka, Croatia
Phone: +385 (51) 770 447
Fax: +385 (51) 686 166
www.intechopen.com

InTech China
Unit 405, Office Block, Hotel Equatorial Shanghai
No.65, Yan An Road (West), Shanghai, 200040, China
中国上海市延安西路65号上海国际贵都大饭店办公楼405单元
Phone: +86-21-62489820
Fax: +86-21-62489821

IntechOpen